Essential Readings in Light Metals: Aluminum Reduction Technology.
Edited by Geoff Bearne, Marc Dupuis and Gary Tarcy.

Light Metals

From *Light Metals 1984*, J.P. McGeer, Editor

PHYSICAL MODELLING OF BUBBLE BEHAVIOUR AND GAS RELEASE FROM ALUMINUM REDUCTION CELL ANODES

S. Fortin, M. Gerhardt, A.J. Gesing

Alcan International Limited
Kingston Laboratories
P.O. Box 8400
Kingston, Ontario
Canada
K7L 4Z4

Abstract

A full-scale model of a two dimensional transverse section through a 150 kA prebake aluminum reduction cell was constructed. Gas evolution on the anode face was simulated by passing air through a porous polyethylene plate. Gas bubble behaviour was photographed and analysed. The effects of current density, anode-cathode distance, and anode tilt and electrolyte velocity on gas layer geometry, anode coverage, bubble velocity, and gas release frequency were investigated. The hydrodynamically produced thick bubble front was observed. Under some conditions, up to 2 cm thick bubble fronts were produced.

Introduction

In the electrolysis of aluminum, aluminum oxide dissolved in electrolyte is dissociated, depositing aluminum in a molten metal pool. Oxygen reacts with the carbon anode and is evolved as CO . CO coalesces into bubbles which then travel to, and are released at, the anode edge. Little is known about the behaviour of the gas bubble layer because of the high temperature and opaque operating environment. The following indirect evidence exists.

During the operation of commercial reduction cells, low amplitude voltage instability is observed at about 1-3 Hz. This frequency correlates well with the frequency of gas bubble release at the anode edge. The electrical and gas release behaviour of the anode indicates that molten electrolyte wets the carbon anode in preference to CO . This is in contrast to fluorine which, when evolved during the anode effect, forms a continuous gas film over the anode and stops the electrolysis.

Static surface tension based calculations predict a CO_2 gas bubble layer thickness of approximately 5 mm. This was confirmed by Haupin's (1) measurements of the voltage gradient in the interpolar space in commercial size reduction cells. In these experiments the electrical signal became very noisy as the voltage probe entered the gas bubble layer, approximately 5 mm from the anode face, and lost contact with the electrolyte as the gas bubbles swept past it. Occasional contact between the probe and the gas bubbles was detected as far away as 2 cm from the anode face.

The gas bubble coverage of the anode face in a 60 kA Soderberg cell operating at a current density of 8 kA/m^2 was estimated by carefully measuring the drop in electrolyte level as the current in an operating cell was turned off. From the knowledge of the freeze profile and the electrolyte level change, it was possible to calculate the volume of gas held-up under the operating anode. Assuming a 5 mm gas bubble thickness, this volume implied that 50% of the anode area was covered by gas bubbles.

Geometry of the anode face is known to affect the behaviour of the gas bubble layer. Specifically, the individual anode size, tilt, and immersion are known to be important. Large vertical stud Soderberg anodes are operated at a smaller current density than prebakes. It is suspected that this is due to the larger gas release path for the V.S. anodes. In horizontal stud anodes, a scalloped anode surface is produced as the carbon is consumed around the slightly inclined stud holes. This, and their generally smaller size, aids the gas release and is presumed to allow operation at current densities approaching that of prebakes. A scalloped anode surface is also sometimes produced by gas channelling under the vertical stud Soderberg anodes. This tends to be induced by operation at a very low anode immersion. It is not clear why low immersion should promote gas channelling. At a normal immersion of 15-20 cm, flat anode faces are observed indicating a uniform average current density over the entire anode face and no gas channelling.

The anode burns off parallel to the average cathode surface (the surface of the molten metal). Distortions of the metal surface in the form of tilting or domes are often produced by magnetic forces. These distortions then are transferred to the anode face, producing permanent anode tilt and the evolved gas is preferentially directed to either the center channel or the sidewall space.

Rounding of anode edges is observed. It has been postulated that this is due to some electrolysis taking place on the vertical immersed portion of the anode. The extent of rounding would thus depend on the anode cathode distance and the anode immersion. Rounding decreases the flat area of the anode, increasing the current density on that portion of the anode. The slope of the rounded portion promotes the gas release along the anode edges.

It is the objective of this study to explore the effects of the variation of the cell operation and geometrical parameters on the gas layer behaviour by studying the behaviour of gas bubbles in a two dimensional room temperature water model of the liquid zone of a reduction cell.

Dimensional Similarity Considerations

Dimensional similarity considerations for an invicid, laminar flow system predict that, with 1:1 geometrical scaling, and equality of kinematic viscosity and surface tension, the bubble sizes and bubble velocities should be equal in the model and the CO_2-cryolite system. Effects of turbulence, current flow through the liquid and magnetic fields are not modelled. These cannot be conveniently simulated and for the purpose of this study are a-priori assumed to have only a second-order effect on the bubble behaviour.

A gas bubble which evolves on the anode face by an electrolytic process is electrically insulating, blocks the electric current from reaching the anode, and locally arrests electrolysis. The bubble can grow when gas evolves along the perimeter of the bubble. This tends to favour the formation of many small bubbles. In contrast, the bubbles evolved by gas passing through a porous plate can continue to grow by the addition of gas through the entire anode-bubble contact surface. This favours the growth of large bubbles. Hence, the porous plate model does not adequately simulate initial bubble formation and growth. However, in both cases, bubble growth by coalescence takes place. It has been observed in this study that this method of growth dominates for large bubbles and that the small bubbles forming on the anode surface do not significantly affect the motion of large bubbles.

Construction of a full-scale, room temperature electrolytic anode model was considered and abandoned on the basis of excessive heat generation. A porous plate anode model was adopted to study the geometry and motion of large bubbles.

A water-air system was chosen for the model. The respective liquid properties are given in Table I:

Table I. Liquid Properties

System	Temperature °C	Density Mg/m^3	Kinematic Surface Tension Dynes cm^2/g	Kinematic Viscosity cpoise cm^3/g
Cryolite	950	2.1	60	1.5
Water	25	1.0	70	1.0

This gives a close match for the kinematic surface and viscosity properties. They were judged to be sufficiently close for the evaluation of the effects of changes in geometrical and operating parameters of the reduction cell.

Apparatus

A full-scale model of a two dimensional, transverse slice of the liquid zone of a 150 kA prebake cell was built. A schematic of the model test section is shown in Figure 1. The model consisted of a glass sided tank, 450 cm long, 61 cm high, and 40 cm wide. The anodes were modelled by suspending two aluminum boxes within the tank. Two anodes were suspended within the tank; each was 135 cm long, 66 cm high, and 40 cm wide. Screw mounting of the anodes permitted the adjustment of both the anode elevation and tilt. Gas evolution was simulated by forcing air through a micro-porous high density polyethylene plate which modelled the anode face. Each anode box was subdivided into fifteen air-tight compartments, 27 cm × 13 cm. Air flow in each compartment was individually controlled to ensure uniform gas distribution over the anode face. Along the long edge of the anode slices, a 2 cm wide lip extended below the polyethylene plate to direct the gas along the long axis of the model. The liquid was circulated through the ends of the model and along an external return circuit by a variable speed propeller pump. The bottom edge of the interpolar space was defined by suspending a transparent 9 mm thick Plexiglas sheet parallel to the face of the anodes, modelling a solid cathode surface with little or no metal on it. The bubble behaviour was observed by placing a mirror below the plexiglas plate.

Experimental

The effect of anode-cathode distance, ACD, was investigated by varying the spacing between the plexiglass "cathode" surface and the porous polyethylene "anode" face. Changes in current density were simulated by varying the air flow rate through the porous polyethylene "anode" plate. Since passage of four electrons through the circuit is necessary to release one molecule of CO_2, there is a strict correlation between the current density and gas flow rate of: $10\ kAm^{-2} = 2.71\ Lm^{-2}s^{-1}$. Effects of changes in liquid velocity and anode tilt were also investigated. A convention was set up so that a positive liquid velocity indicates that liquid flow is co-current with the gas bubble motion. Table II gives the range of variation of each parameter. Anode immersion was kept constant at 15 cm.

Table II. Range of Variation of Experimental Parameters

Current Density ($kA\ m^{-2}$)	Liquid Velocity ($cm\ s^{-1}$)	Anode-Cathode Distance (cm)	Anode Tilt (degrees)
4.3	-16.7	3	0
8.7	- 8.0	5	0.43
	- 3.6		1.07
	.0		2.58
	3.6		
	8.0		
	16.7		

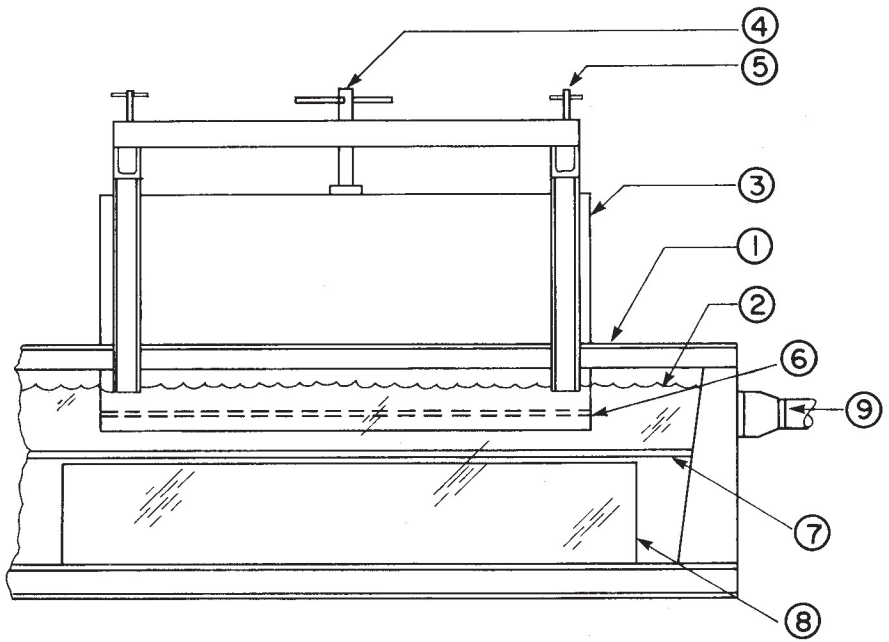

Figure 1 - Schematic of the water model of the aluminum reduction cell: (1) water tank, (2) water level, (3) anode, (4) anode height adjustment, (5) anode tilt adjustment, (6) porous polyethylene, (7) plexiglas plate, (8) mirror, (9) water circulation nozzle.

Measurements were videorecorded as follows. A projection of the bubbles on the anode face was recorded from a mirror inclined at 45° located under the anode. Vertical profiles of the bubbles were recorded just below the anode face with the camera at a nearly horizontal angle. Recordings for each experimental condition were made at two locations - at the centre of the anode and at the anode edge.

Videotapes were then played back in stop-motion and measurements were actually made on the T.V. monitor. The dimensions were scaled to life size by including, in each scene, a square of known dimensions. The time scale was verified by videotaping a stop watch for one minute prior to each experiment.

The measured responses included bubble geometry, gas bubble coverage of anode area, bubble velocity, and frequency of bubble release at the anode edge. Bubble geometry was characterized by the measurement of overall dimensions along and transverse to the direction of bubble motion as well as the height and width of the dynamic bubble front formed at the leading edge of the large bubbles. The model anode was designed such that its long edge extends 2 cm below the anode face. Bubble heights were obtained by videotaping at a nearly horizontal angle and measuring the bubble profiles projected against the extension on the far side of the anode as illustrated in Figure 2.

Average dimensions for five large bubbles are quoted for each experimental condition. Gas bubble velocity was calculated by timing the motion of the bubble between two fixed points. The percent of the anode face covered by gas was calculating by using a 440 square section grid and determining the fraction of the intersection points that were over the gas bubbles. In order to avoid aliasing the data, the average coverage for equally spaced time intervals within one bubble cycle is reported.

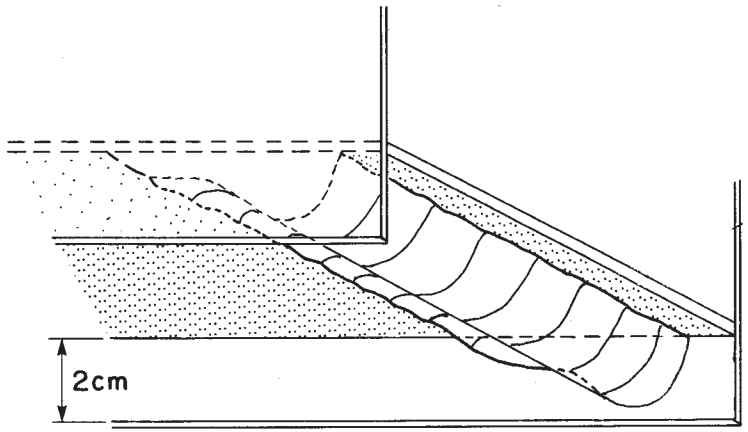

Figure 2 - Gas bubble flowing beneath the porous plate from left to right. Bubble profile, 1, is seen against the extended anode edge, 2.

Results

Bubble Behaviour on a Horizontal Anode Surface

The anode face was judged to be horizontal when, with stationary liquid, no motion of growing bubbles was observed. In this case, small spherical bubbles were generated on the entire anode surface. They grew to a diameter of ~5 mm before expanding horizontally. They coalesced into large individual bubbles until they covered approximately 50-60% of the anode area. At that time they impinged on each other and simultaneously coalesced into a single bubble covering the entire anode face. The edge of the gas sheet almost immediately reached the anode edge and the gas escaped from the anode face with the speed of the air leaving a broken balloon. Clean anode surface was left ready to repeat the process. This process is illustrated in Figure 3.

In this process the time averaged percentage of the anode area covered by gas bubbles was observed to be independent of current density (air flow rate). The gas bubble release frequency increased with the current density. The liquid motion did not alter the overall process. The bubbles were swept slowly towards the downstream edge of the overall anode causing most of the bubble release to take place there.

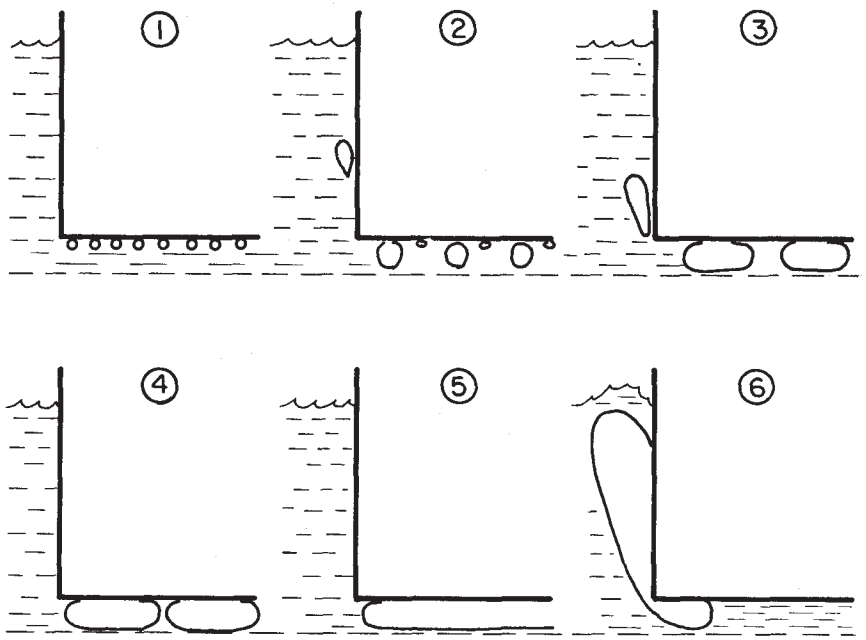

Figure 3 - Steps in the gas release cycle from a horizontal anode face. (1) Formation of bubbles, (2) spherical growth, (3) lateral spread, (4) mutual impingement, (5) coalescence into a single gas sheet, (6) gas release at the anode edge leaving a clean anode surface.

As the coalesced gas layer was released from the edge of the anode all at once, the liquid was sucked into the interpolar gap to replace the gas. The gas bubble rising through the liquid up the anode side created a pumping action which vigorously stirred the anode-sidewall and anode-anode gaps. The result is that the bulk of the disturbance caused by gas bubbles was created at the anode edge and very little underneath the anode. This was particularily evident when a second liquid was used to model the molten pool cathode. Waves were generated on the liquid-liquid interface at the anode edge. They then travelled under the anode.

Bubble Behaviour on the Tilted Anode Surface

Anode tilt drastically affected the behaviour of the bubble layer. A tilt of a fraction of a degree was sufficient to induce significant buoyancy driven motion of the gas bubbles. Examples of typical bubble patterns are shown in Figures 4 to 7.

Small bubbles were created on the entire anode surface. These small bubbles moved slowly. As they began to coalesce they gained velocity. This caused the "sweeping" effect shown in Figure 6 as the large bubbles travelled along the anode face overtaking and swallowing any small bubbles they came into contact with. Bubble growth was rapid and continuous with the bubble gaining in size and speed until it was released at the anode edge. Coalescence of all the bubbles into a continuous layer no longer took place, but a characteristic bubble pattern was developed. This pattern depended on anode tilt, liquid velocity, current density, and location on the anode face.

As the bubble velocity increased, the ratio of transverse to longitudinal dimensions of the bubble increased promoting bubble coalescence in a transverse direction and increasing the separation between successive large bubbles. In many cases this resulted in two dimensional bubbles spanning the entire width of the model section of the anode. The leading edge of the large bubble was preceded by a layer of small bubbles about to coalesce with it. The trailing edge swept the area behind it clean, ready for the formation of new small bubbles.

The shape of a moving bubble was no longer limited by static surface tension balance. The typical bubble profile is shown in Figure 8(A). The thickness of the front portion of the bubble increased in size. As the bubble surface became horizontal the bubble front collapsed, and the trailing portion of the bubble had a thickness similar to those observed at static conditions. In the case of large fast moving bubbles, secondary wavelets were formed along the gas-liquid interface of the trailing portion of the bubble.

Effect of Anode-Cathode Distance. In all cases, a change of ACD from 5 to 3 cm had no effect on the bubble patterns or on any of the measured responses. However, it is interesting to note that the large gas bubbles passing over the Plexiglas sheet, which simulated the cathode, caused enough disturbance to shake the 9 mm thick sheet. This disturbance was more noticeable at the low ACD.

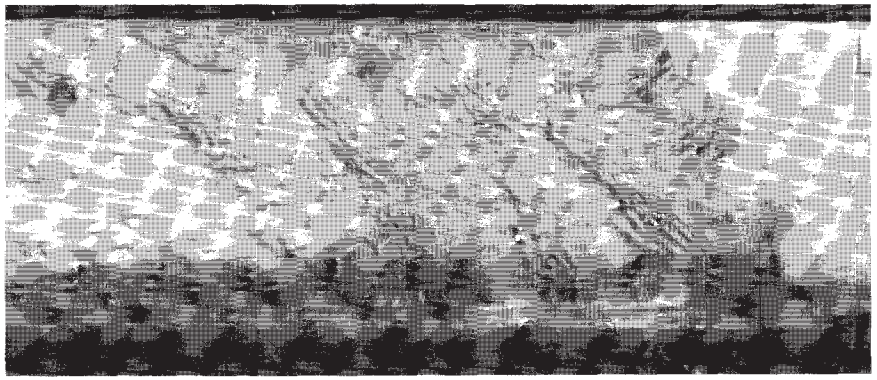

Figure 4 - A bubble covering almost the entire anode face is formed on a nearly horizontal anode with a countercurrent liquid flow.

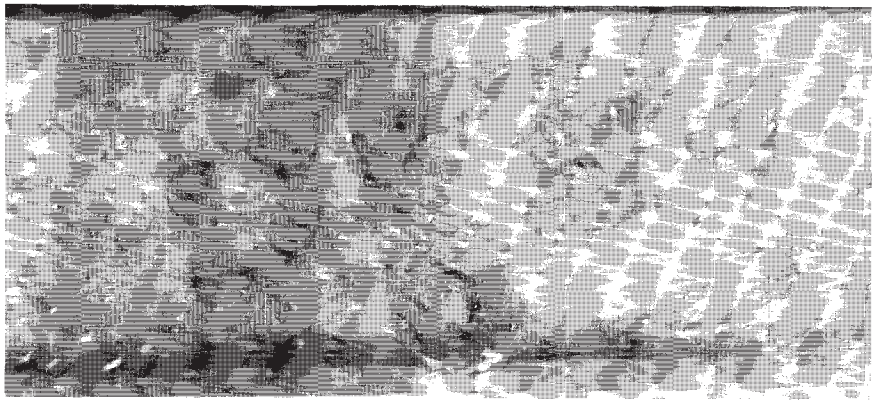

Figure 5 - Gas bubbles growing and coalescing at the center of the anode while travelling from left to right.

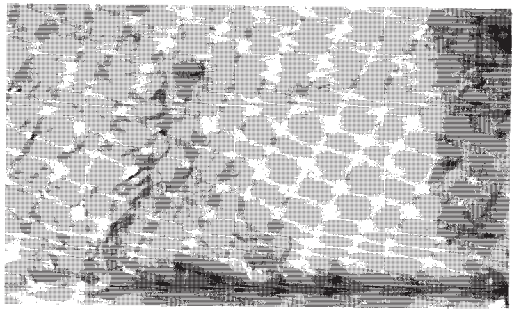

Figure 6 - Sweeping action of the large bubbles as they move from right to left.

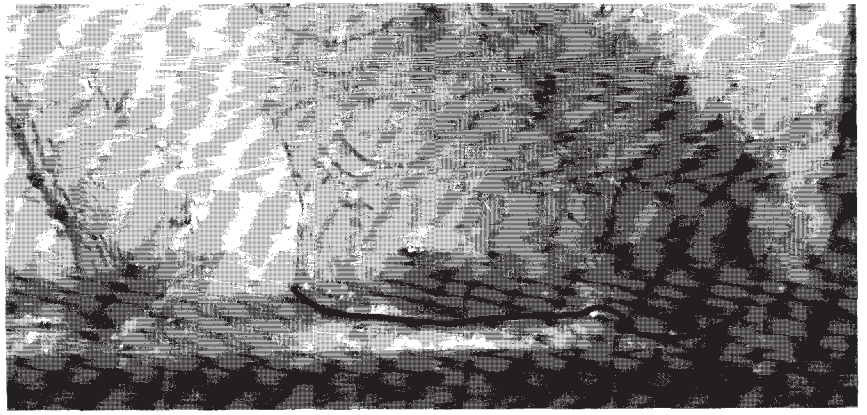

Figure 7 - Large bubble travelling from right to left. A high bubble front if visible and the bubble profile is outlined against a 2 cm wide anode edge extension.

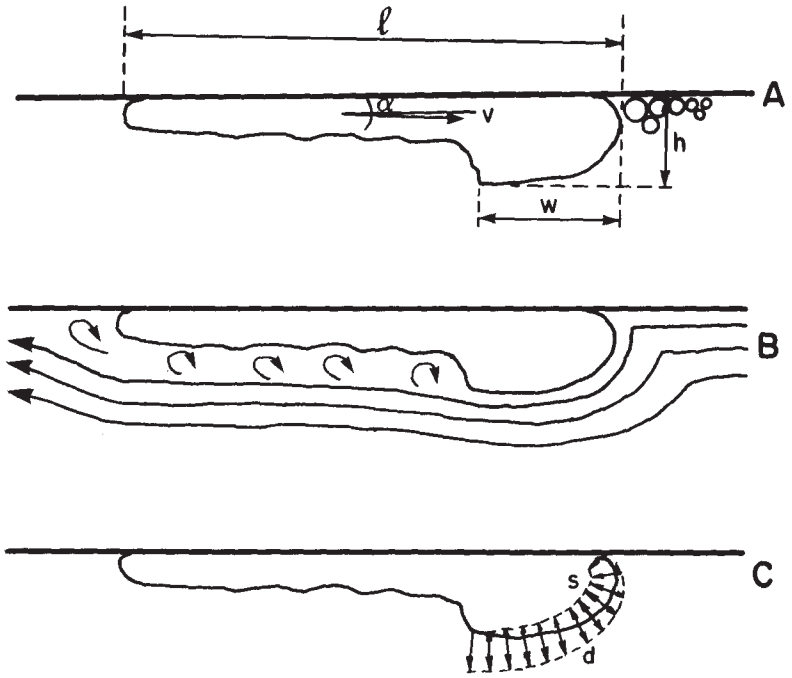

Figure 8 - (A) Typical profile of a large bubble travelling up the anode slope. (B) Streamlines generated by the relative motion of the bubble and the electrolyte. Boundary layer separation occurs at the aft end of the bubble front resulting in the turbulent region downstream. (C) Hydrostatic, s, and hydrodynamic, d, pressure distributions along the bubble front.

Longitudinal Dimension of the Bubbles. This dimension was measured parallel to the direction of bubble motion at the center of the anode. The "length" varied from 2 to 128 cm. It increased with an increase in current density and decreased with increase in liquid velocity or anode tilt as shown in Figure 9.

Transverse Dimensions of the Bubbles. The bubble dimension perpendicular to the direction of motion varied from 4 to 40 cm (the entire width of the anode slice) when measured at the center of the anode. For any bubble not spanning the entire anode slice, this "width" was larger than the corresponding "length" measured parallel to the direction of motion. Figure 10 shows that bubble "width" increased with an increase in current density. At high countercurrent liquid velocities, an increase of anode tilt caused a large decrease in the bubble "width". Tilt had negligible effect on bubble "width" when liquid was flowing in cocurrent direction.

Bubble Profile. The shape of the bubble profile consisted of a thick bubble front and a thin (~5 mm), long trailing portion. Bubble front thickness and width are both defined in Figure 8(A). They were measured for two dimensional bubbles near the edge of the anode at the intersection of the bubble and the extended anode edge. The bubble front thickness varied between 0.8 and 2.4 cm. An increase in current density increased the thickness while an increase in liquid velocity decreased it. Figure 11(A) shows these effects while Figure 11(B) illustrates the effect of anode tilt. With the liquid flowing in a countercurrent direction, an increase in anode tilt caused an increase in front thickness. With a cocurrent flow, an incresed tilt decreased the front thickness slightly.

The measurements of the width of the bubble front illustrated in Figure 12 ranged from 0 to 14.5 cm. An increased front width was recorded with increased current density and anode tilt. An increase in liquid velocity decreased the front width. The effect of the velocity was much more pronounced at a high tilt.

Percent of Anode Area Covered by Gas. In the case of the tilted model anode, the bubble size and the amount of gas passing a given point increased from the low to high edge of the anode. The coverage values were measured at the center of a tilted model anode. The bubble coverage varied from a low of 24% to a high of 90%. The amount of bubble coverage decreased with the increase in liquid velocity and increased with an increase in current density. The anode tilt results depended on liquid velocity and the ACD had no effect.

An increase in current density caused an increase in bubble coverage. The amount of coverage, however, was not proportional to the volume of gas being passed through the anode. Figure 13(A) shows that when current density was doubled, the bubble coverage increased by 10-22%.

The effect of the anode tilt on bubble coverage depended on the direction and magnitude of liquid velocity. Figure 13(B) shows that at a high countercurrent liquid velocity of -16.7 cm/s, an anode with a low tilt of 0.43° had 27% more area covered by gas than an anode with a high tilt of 2.58°. However, at a high cocurrent liquid velocity of 16.7 cm/s there was no significant effect of tilt on coverage.

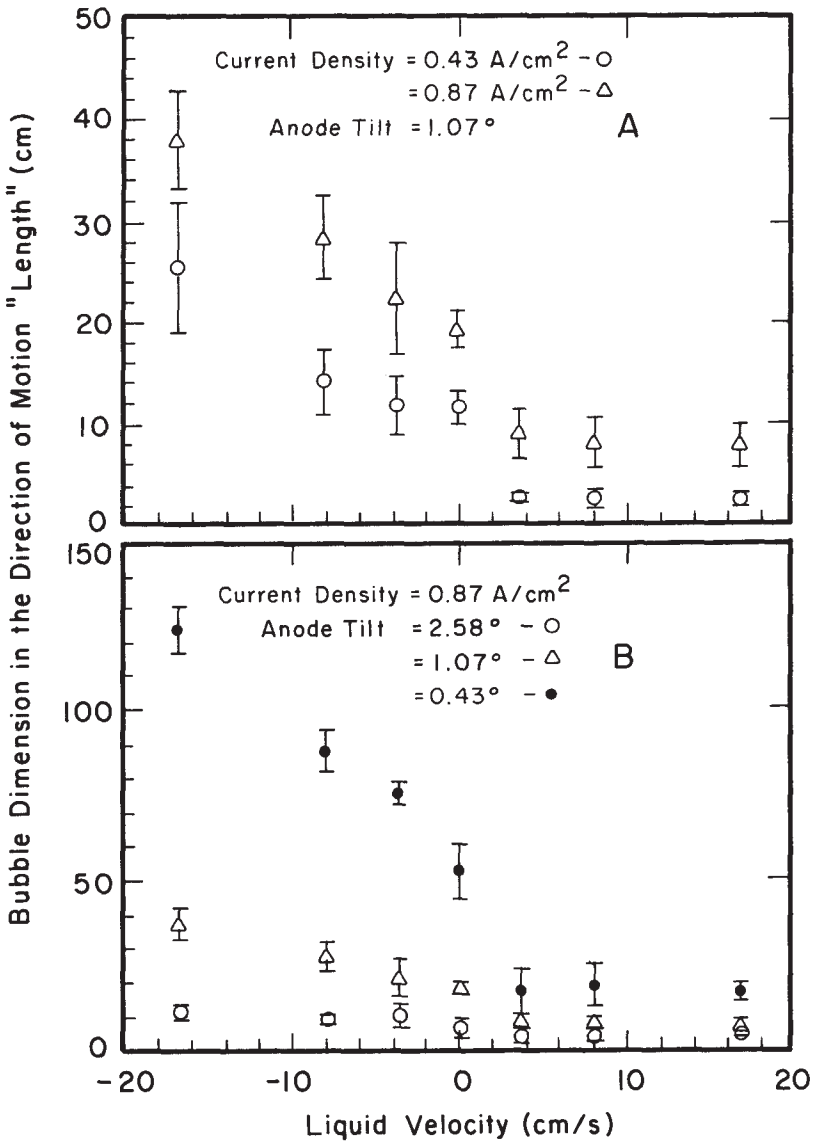

Figure 9 - Effects of liquid velocity, current density, and anode tilt on the gas bubble "length".

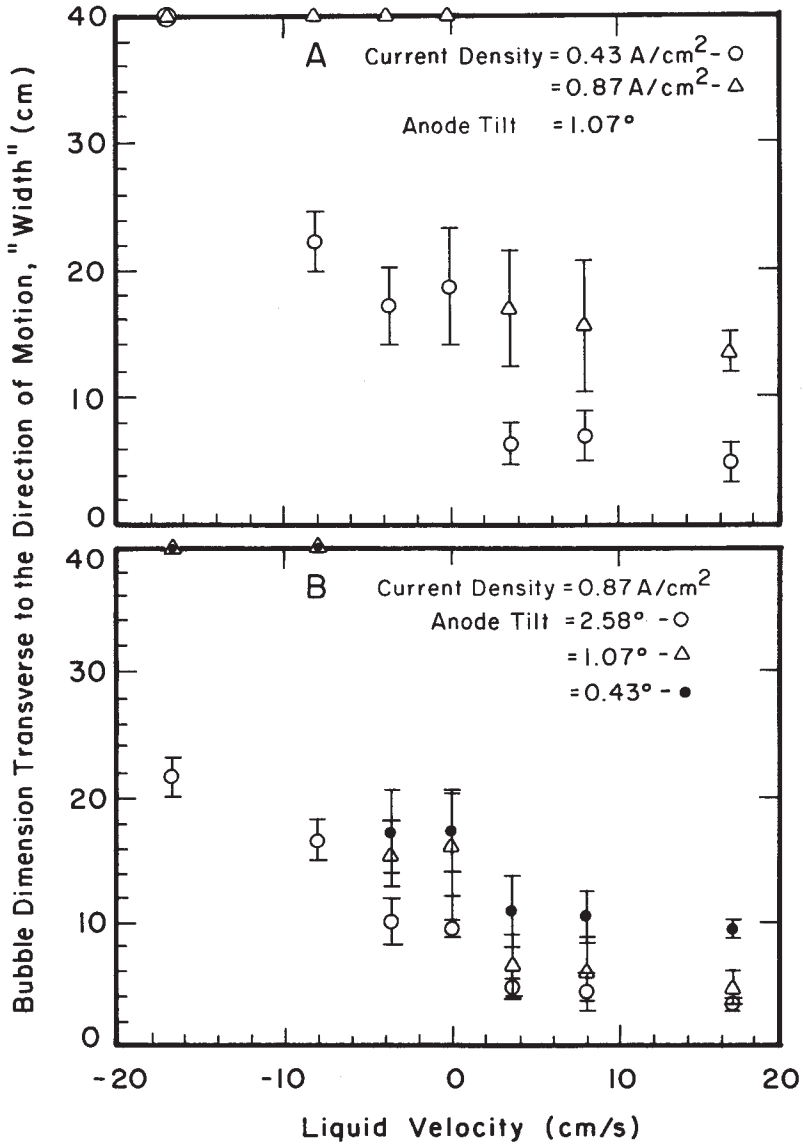

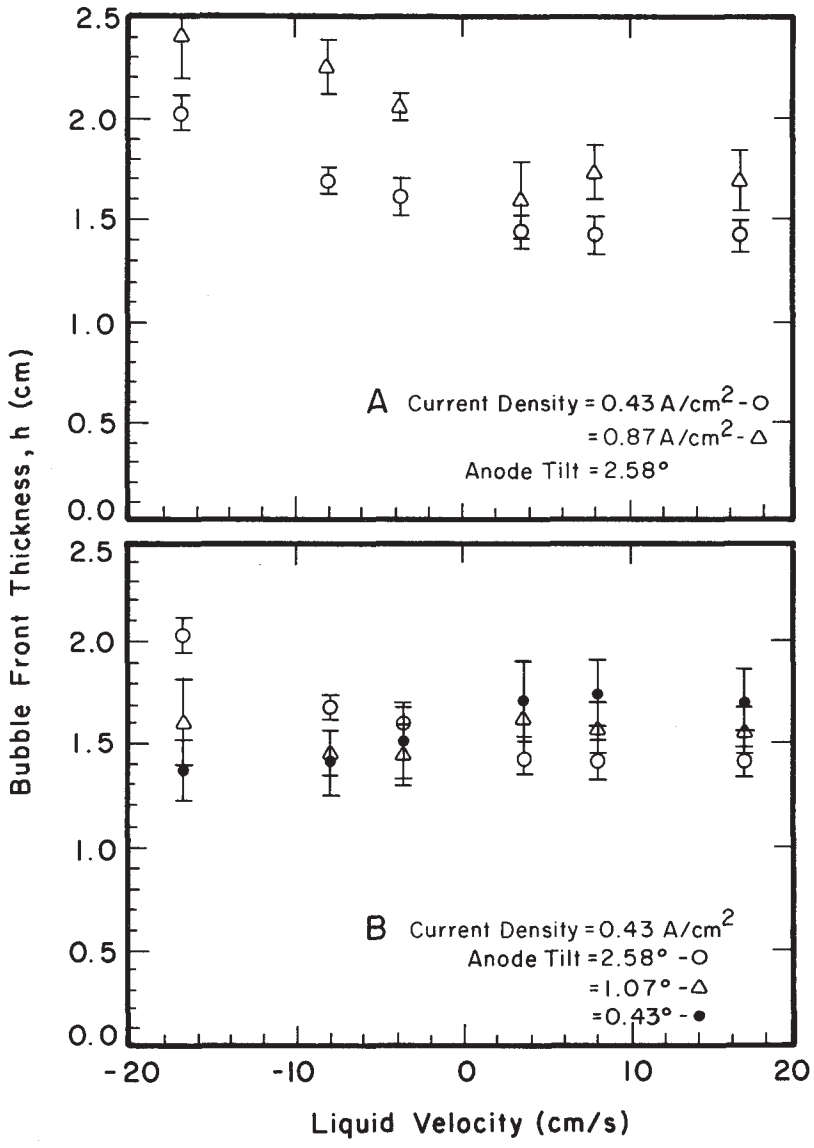

Figure 10 - Effects of liquid velocity, current density, and anode tilt on the gas bubble "width".

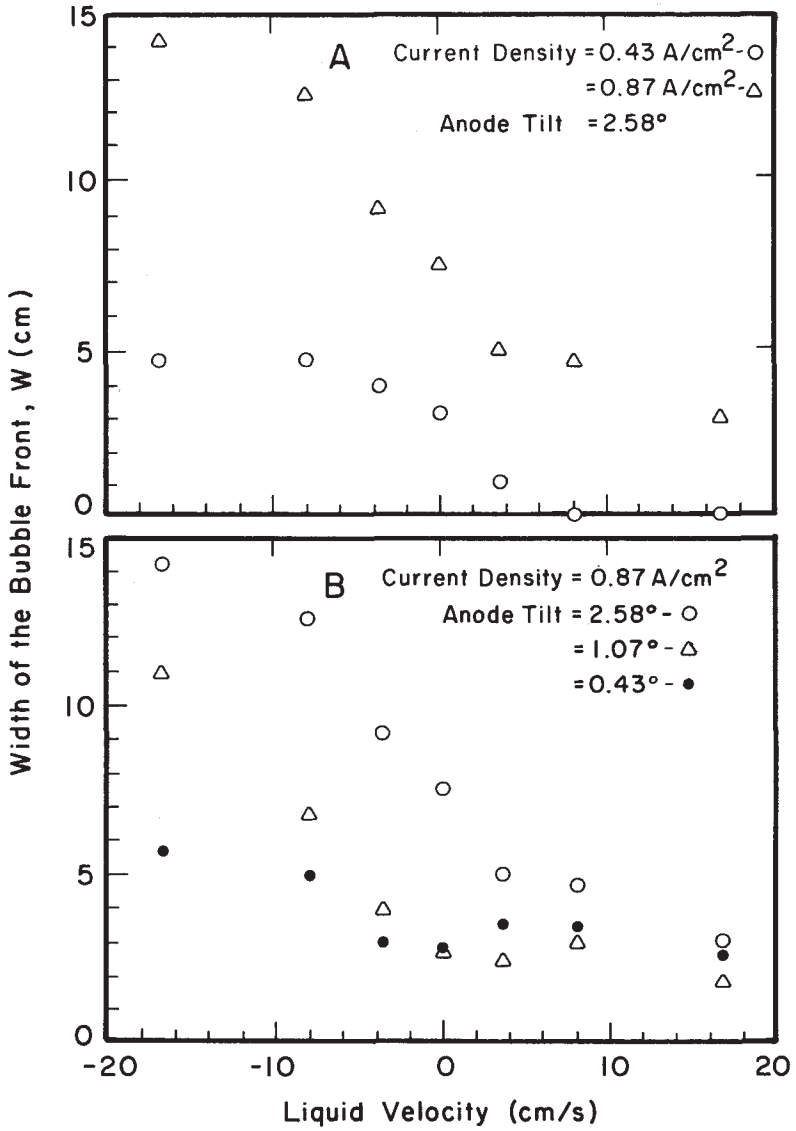

Figure 12 - Effects of liquid velocity, current density, and anode tilt on the width of the gas bubble front.

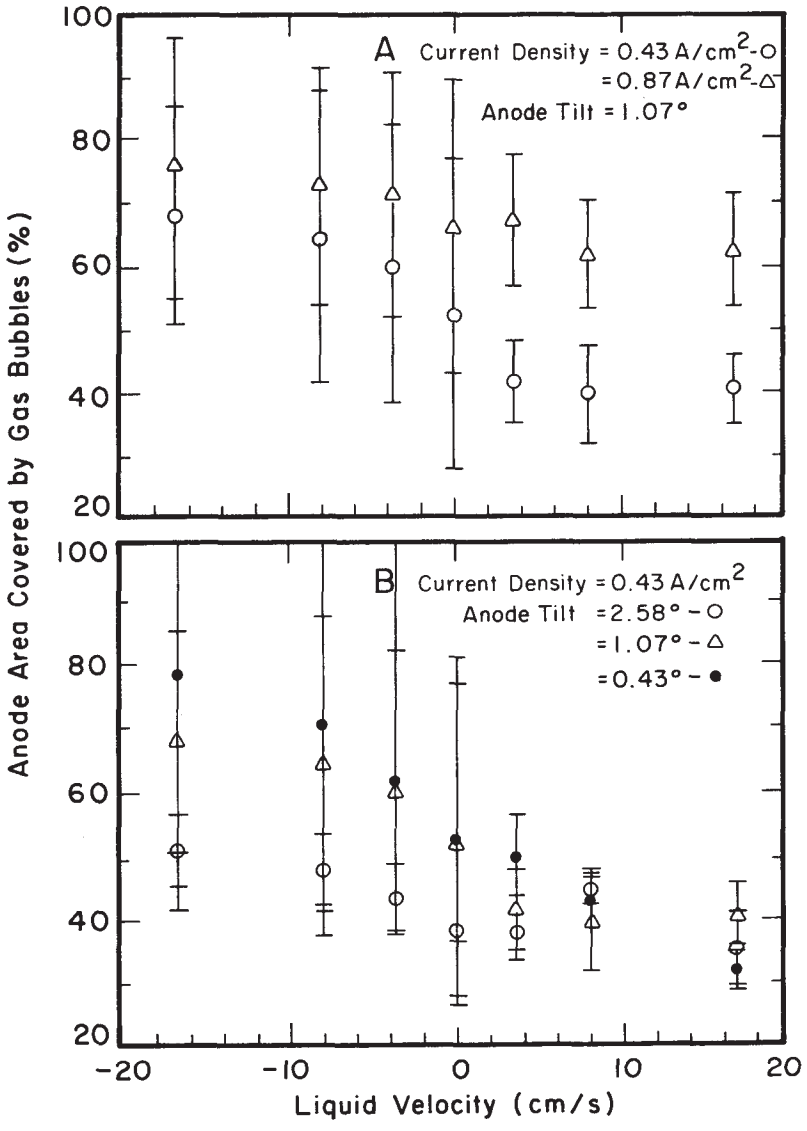

Figure 13 - Effects of liquid velocity, current density, and anode tilt on the percentage of anode area covered by gas bubbles.

Gas Bubble Velocity. With a low anode tilt and the liquid flowing in a countercurrent direction, small bubbles moved down the anode slope. As they grew in size, and they reversed direction and traveled up the anode face. The larger bubbles caught up to and coalesced with the smaller ones. An apparent jump in the velocity of the bubble leading edge occurred when several similarly sized bubbles traveled up the anode together. They grew until at one point they impinged on each other and suddenly coalesced into a single bubble. This registered as a sudden apparent increase in the velocity of the leading edge of the largest bubble. Another anomaly occurred when the leading edge reached the edge of the anode. As the air escaped over the edge, the velocity of the trailing edge of the bubble increased dramatically.

The gas bubble velocities observed at the center of the anode were in the range 8 to 40 cm/s. Bubble velocity increased with an increase in liquid velocity or current density. Both the ACD and anode tilt had only a limited effect. The increase in gas bubble velocity was 10-16 cm/s as the liquid velocity was increased from -16.7 to 16.7 cm/s. The curve has a definite "S" shape with the slope being higher at a slow liquid speed and lower at a high liquid speed (both cocurrent and countercurrent). An increase in current density caused an increase in the gas bubble velocity. Figure 14(A) shows that the bubble velocity is consistently 5 to 13 cm/s faster at a current density of 8.7 kA/m^2 than at 4.3 kA/m^2. Surprisingly, the anode tilt had very little effect on the gas velocity. Figure 14(B) shows that the difference in the bubble velocity on tilts of 0.43° and 2.58° never exceeds 3 cm/s.

Bubble Release Frequency. Bubbles were released from the edge of the anode at frequencies ranging from 0.2 to 3.3 bubbles per second. The frequency increased with an increase in either liquid velocity or anode tilt. The current density and ACD had no effect on the frequency. Figure 15(A) shows that an increase in the liquid velocity from -16.7 to 16.7 cm/s caused an increase in frequency of between 1.4 and 2 s^{-1}.

Conclusions

Table III summarizes the results obtained in this study. The ACD had no effect on gas bubble behaviour. An increase in current density increased the bubble size and thickness of the bubble front as well as gas coverage of the anode face and bubble velocity. Current density had no effect on bubble release frequencies. An increase in electrolyte velocity decreased the bubble size and the gas coverage and increased the bubble velocity and release frequency. An increase in anode tilt decreased the bubble size and gas coverage and increased the bubble release frequency. Tilt had no effect on bubble velocity. There was considerable interaction between the effects of the experimental variables on bubble size and bubble velocity.

Behaviour of the gas layer on a horizontal anode was different than on an inclined anode. On a horizontal anode, the process of bubble nucleation, growth, coalescence and release involved no bubble motion and led to a gas layer thickness of approximately 5 mm. On the inclined surface, gas behaviour was dominated by the motion of large bubbles across the anode surface. Hydrodynamic effects increase the maximum thickness of the bubbles to more than 2 cm. The results of this study are in very good agreement with indirect measurements on the aluminum reduction cells published to date (1).

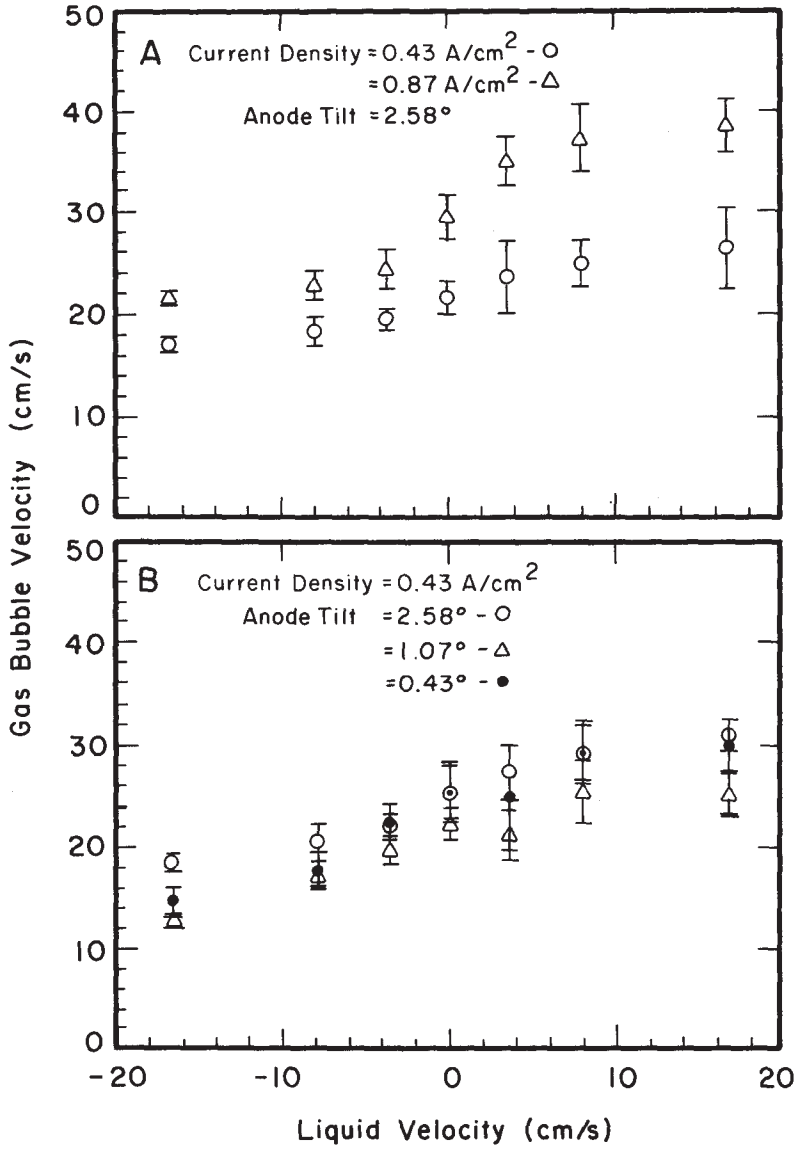

Figure 14 - The effects of liquid velocity, current density, and anode tilt on the gas bubble velocity.

Table III. Average Slope of the Graph of Response Parameter Against Experimental Variables

Response Parameter \ Experimental Variable	Current Density, i (kA/m^2)	Electrolyte Velocity, v (cm/s)	Anode Tilt, α (degrees)	Range of Values Observed
Longitudinal dimension of the bubble (cm)	2.8 @ v = -16.7 2.2 @ v = 0 1.1 @ v = 16.7	-3.3 @ α = 0.4° -1.0 @ α = 1.1° -0.4 @ α = 2.6°	-52 @ v = -16.7 -22 @ v = 0 -5.6 @ v = 16.7	2-128
Transverse dimension of the bubble (cm)	2.0 @ v > 0	-0.6 @ v > 0	-2.8 @ v > 0	4-40
Bubble front height (cm)	+0.1	+0.01 @ α = 0.4° +0 @ α = 1.1° -0.02 @ α = 2.6°	+0.33 @ v = -16.7 0 @ v = 0 -0.14 @ v = -16.7	0.8-2.4
Bubble front thickness (cm)	~1.0-2.0	-3.3 @ α = 2.6° -0.9 @ α = 0.4°	4.0 @ v = -16.7 0 @ v = 16.7	0-14.5
Anode area covered by gas (%)	+3.6	-0.65	-12.1 @ v = -16.7 -7.4 @ v = 0 0 @ v = 16.7	24-90
Bubble release frequency (s^{-1})	0	+0.04	+0.72	0.3-3.3
Bubble velocity (cm/s)	+1.0 @ v = -16.7 +1.8 @ v = 0 +2.7 @ v = 16.7	+0.4	0	8-46

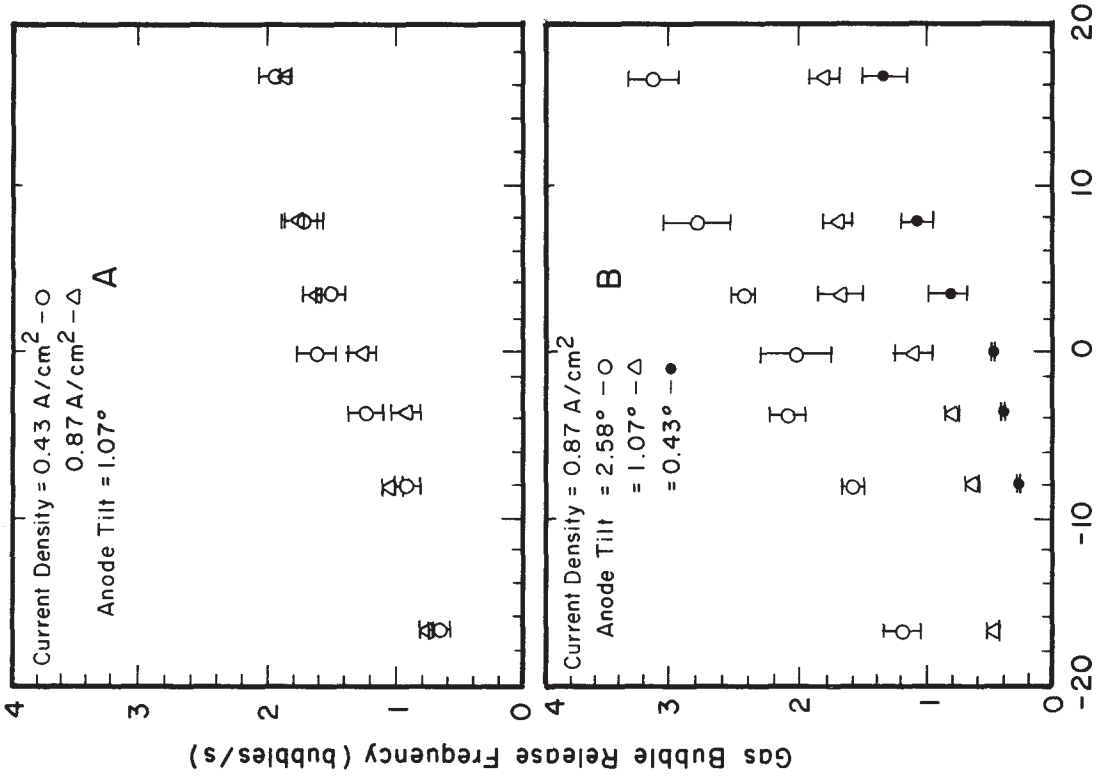

Figure 15 - Effects of liquid velocity, current density, and anode tilt on the gas bubble release frequency.

Acknowledgements

This work is an extension of physical modelling of aluminum reduction cells carried out at Alcan by T. Cambridge and E. Dernede. The measurements of gas coverage in operating the 60 kA Soderberg cells were performed under supervision of O. Sivilotti. M. Schneider and G. Quinn were instrumental in the design and construction of the physical model.

References

(1) W. Haupin, A Scanning Reference Electrode for Voltage Contours in Aluminum Smelting Cells, Journal of Metals. 23 (10) (1971), pp. 46-49.

(2) I.H. Abbott and A.E. VonDoenhoff, Theory of Wing Sections, Dover Publications, New York, New York, 1958.